

Reduction and Biosorption of Cr(VI) from Aqueous Solution Using Cellulose Microfibers Obtained from Cardboard Waste

Karina Piedra-Ambriz¹, Ruth Alfaro-Cuevas-Villanueva², Raúl Cortés-Martínez^{2*}

¹MSc Environmental Engineering Program, Facultad de Biología, Universidad Michoacana de San Nicolás de Hidalgo, Morelia, Michoacán, México.

²Earth Sciences Research Institute, Universidad Michoacana de San Nicolás de Hidalgo, Morelia, Michoacán, México.

*Corresponding Author

ABSTRACT

The environmental persistence and toxicity of hexavalent chromium [Cr(VI)] pose significant risks to ecosystems and human health, demanding innovative remediation strategies. This study investigates the reduction and biosorption of Cr(VI) from aqueous solutions using cellulose microfibers (MFCs) synthesized from corrugated cardboard waste. The study's objective was to synthesize, characterize, and evaluate the efficiency of MFCs in removing Cr(VI), exploring the mechanisms and conditions that optimize the process. MFCs were synthesized through a multi-step chemical and mechanical treatment process, resulting in a material with high surface area and functional groups conducive to Cr(VI) adsorption. Scanning Electron Microscopy (SEM) and Fourier Transform Infrared Spectroscopy (FTIR) analyses confirmed the morphological and chemical characteristics of the MFCs, while zeta potential measurements provided insights into surface charge behavior across pH levels. Experimental results demonstrated that the MFCs achieved a maximum % Cr(VI) removal efficiency of 60% under optimal conditions. Kinetic studies revealed rapid adsorption within 60 minutes, with equilibrium established afterward. The biosorption efficiency was significantly influenced by pH, with the highest removal observed in acidic conditions (pH 2–4), attributed to favorable electrostatic interactions and redox processes. The maximum Cr(VI) adsorption capacity was approximately 900 mg Cr(VI)/g MFC at 35°C. Increasing the biosorbent dosage improved removal efficiency, while temperature variation suggested an optimal range of 25–35°C for maximum biosorption. FTIR analyses indicated that functional groups, such as hydroxyls and carboxyls, actively participated in Cr(VI) adsorption and reduction to the less toxic Cr(III). The isotherm studies highlighted the adsorption capacity of MFCs, making them a sustainable alternative to conventional adsorbents. This study underscores the potential of utilizing waste-derived MFCs as cost-effective, environmentally friendly biosorbents for Cr(VI) remediation. Further optimization and scaling could enhance their applicability in treating industrial effluents and contribute to circular economy practices.

Date of Submission: 03-12-2024

Date of Acceptance: 14-12-2024

I. INTRODUCTION

Heavy metal pollution is one of the most critical environmental problems worldwide due to its high toxicity, environmental persistence, and capacity for bioaccumulation in living organisms. Heavy metals like lead, mercury, cadmium, and arsenic accumulate in the environment, leading to biomagnification and posing significant ecological and human health risks. Heavy metals are released into the environment through industrial processes such as mining, smelting, and manufacturing. These activities contribute significantly to soil and water contamination [1,2]. Ecological effects of heavy metals include adverse effects on soil microbial populations and plant growth, leading to reduced agricultural productivity and biodiversity loss [1,3]. Human health risks include cancer, respiratory ailments, and reproductive defects, particularly in children. Food chain contamination occurs through contaminated water and soil, posing risks to wildlife and humans [2,4].

Among these pollutants, hexavalent chromium [Cr(VI)] is classified as one of the priority substances due to its harmful impact on human health and aquatic ecosystems. This metal is widely used in industrial processes such as electroplating, leather tanning, pigment manufacturing, and metal treatment, generating large amounts of contaminated effluents. Cr(VI) exposure can cause mutagenicity, teratogenicity, and carcinogenicity, affecting vital organs such as the liver and kidneys. It can penetrate biological membranes and enter cells, where

it is reduced to Cr(III), generating reactive oxygen species (ROS) that cause oxidative stress and cellular damage [5]. Cr(VI) is highly soluble and mobile, making it a persistent contaminant in aquatic environments. It can interfere with photosynthesis, seed germination, and plant nutrient uptake, affecting overall plant growth and ecosystem functionality [6]. The natural occurrence of Cr(VI) in specific geological settings, such as areas with ophiolite rocks, further complicates its management and demands an understanding of its natural background levels for effective regulation. Regulatory agencies like the United States Environmental Protection Agency (U.S. EPA) have established guidelines to limit Cr(VI) concentrations in drinking water to protect public health. The MPL for Cr(VI) in drinking water is typically set at 10 ppb or 0.01 mg/L in the United States, reflecting its classification as a priority pollutant due to its adverse health effects [7,8].

Removing Cr(VI) from contaminated water poses a significant challenge for existing treatment technology. Traditional techniques, including chemical precipitation, activated carbon adsorption, membrane filtration, ion exchange, and sophisticated oxidation processes, have demonstrated efficacy but have severe limitations. These include high operating costs, generation of secondary waste, and variable efficiency under different environmental conditions. For instance, chemical reduction and precipitation generate large sludge volumes, leading to secondary pollution if not managed properly [9]. Ion exchange systems have high initial costs and require careful pH and ionic strength control [10]. Membrane filtration is energy-intensive and may not be cost-effective for large volumes of wastewater [10]. Electrochemical processes are expensive due to high energy requirements and specialized equipment, and their effectiveness can be influenced by initial Cr(VI) concentration and other ions. These facts have motivated the search for more sustainable and economical alternatives that take advantage of abundant and low-cost materials.

Among these methods, adsorption is considered one of the most effective methods for removing hexavalent chromium from water due to its high efficiency, cost-effectiveness, and versatility, especially at low concentrations [11]. This method utilizes various materials that can be modified to enhance their adsorption capabilities and mechanisms, making it suitable for diverse water treatment applications. Furthermore, in some cases, Cr(VI) is reduced to the less toxic Cr(III), allowing for the recovery of chromium [12]. Adsorption uses various adsorbents, such as carbon nanotubes, graphene oxide, and biochars, and is economically viable due to the use of low-cost materials. Adsorption processes often involve multiple mechanisms, such as electrostatic attraction, ion exchange, and chemical complexation, which improves removal efficiency. Adsorption is also environmentally friendly, as it uses natural or modified materials, reducing the environmental impact compared to other chemical treatments.

In this context, biomass-based materials are increasingly recognized as effective adsorbents for pollutant removal due to their availability, low cost, and favorable physicochemical properties. In particular, cellulose nanofibers (CNFs), derived from lignocellulosic waste, offer unique advantages due to their high surface-to-volume ratio, adaptable surface functionality, and strong bonds with heavy metals [13]. These properties make them ideal for environmental remediation applications. However, their potential for Cr(VI) reduction and removal has not been thoroughly explored, mainly when obtained from paper waste, an abundant and underutilized resource in many countries. Paper waste represents an economical and sustainable source for obtaining cellulose nanofibers, promoting the circular economy, and reducing the pressure on natural resources [14]. Cellulose, the main component of paper waste, can be transformed into nanofibers through hydrolysis and controlled machining processes, generating materials with specific characteristics that improve their adsorbent and reducing capacity. Recent studies have shown that modifying the surface of nanofibers by introducing functional groups such as carboxyls or hydroxyls can increase their affinity for metal contaminants by facilitating adsorption and chemical reduction processes [15]. Based on these observations, we hypothesize that cellulose microfibers obtained from cardboard waste can be an efficient and sustainable biosorbent for reducing and removing Cr(VI) in aqueous solutions due to their high surface area, chemical functionality, and chemical reduction capacity. In this study, we aim to investigate the potential of cellulose microfibers not only as adsorbents but also as reducing agents that can transform Cr(VI) into less toxic forms. This approach could mitigate the environmental impact of this pollutant in aquatic environments.

Thus, this study aimed to synthesize and characterize cellulose microfibers from cardboard waste, evaluate their properties, and determine their capacity to reduce and adsorb Cr(VI) under controlled conditions. The basic parameters of kinetics and equilibrium were assessed, as well as the pH and temperature effect on the chromium removal.

II. MATERIAL AND METHODS

This section presents the phase-wise description of the developed risk-impact assessment methodology.

2.1. Cardboard residues pretreatment

Corrugated cardboard waste was collected, previously cut into medium-sized pieces and washed with distilled water to remove impurities. This material was soaked for 24 hours in a container with distilled water.

Finally, it was dried at room temperature and manually cut into small pieces for later use in obtaining cellulose microfibers.

Prior to obtaining cellulose microfibers, a chemical treatment was carried out on the pretreated cardboard, based on a previously proposed method [16], which is summarized below: The sample was treated with 2% NaOH at 90°C for 2 hours to leach ink and hemicellulose. Then, it was treated with 25 g of sodium chlorite solution with 200 mL of acetic acid in 1 L of water at 75°C for 1 hour to eliminate lignin residues. It was treated with 2% KOH at 90°C for 2 hours to eliminate ink and hemicellulose residues further. In order to obtain a pure sample, the sample was subjected to an additional treatment with 25 g of sodium chlorite, 200 mL of acetic acid, and 1 L of water at 75 °C for 1 hour. Finally, it was treated with 5% (w/w) KOH at 90 °C for 2 hours. Throughout the process, the sample was washed with deionized water until it reached a neutral pH, maintaining its swollen state at all times.

2.2. Cellulose microfibers (MFCs) synthesis

The samples obtained from cardboard pretreatment were dried overnight in an oven at 35°C to remove all moisture. They were then subjected to several grindings using a blender to obtain a material with a smaller particle size, close to a pulverized material. Once again, the obtained sample was dried for 24 hours at 25°C. Finally, the MFCs were fibrillated by grinding with liquid nitrogen, as reported in our previous works [13,15].

2.3. MFCs characterization

Cellulose microfibers (MFCs) obtained from corrugated cardboard waste were characterized by different methods to determine their morphology, size, surface chemistry, and electrostatic properties. Firstly, Scanning Electron Microscopy (SEM) analyses were performed, where the MFCs were coated with copper and studied with a JSPM-5200 scanning electron microscope and a JEOL JSM-7600F FEG-SEM microanalysis detector (EDS analysis) to determine the samples' surface morphology and semi-quantitative elemental analysis.

Subsequently, FTIR analyses were conducted on MFCs. For the measurement, 0.3 g of dry KBr was combined with 0.02 g of each biosorbent sample and subsequently compressed with a force of 3 tons for 1 minute. The samples were examined using a Bruker Tensor 27 FTIR spectrophotometer. The utilized frequency range was from 200 to 4000 cm^{-1} .

Finally, the isoelectric point or point of zero charge (pH_{PZC}) of the MFCs was determined by assessing the zeta potential with a Zeta-Meter System 3+. Multiple biosorbent solutions were prepared at pH values between 2 and 9, with solution adjustments made using 0.01 M HCl and 0.01 M KOH. These tests were conducted at 25 °C.

2.4. Kinetic experiments

Batch tests were conducted to assess the kinetics of Cr(VI) elimination using MFCs. 10mL aliquots of a 10 mg/L potassium dichromate ($\text{K}_2 \text{Cr}_2 \text{O}_7$) solution and 0.1 g of MFCs were placed in centrifuge tubes and agitated at 100 rpm for different contact times (ranging from 5 min to 8 h) at a constant temperature of 25°C. Subsequently, the samples underwent centrifugation and filtration to separate the aqueous phase, which was subsequently tested for Cr(VI) by UV-Vis and total chromium using an atomic absorption spectrometer (AAS). The Cr(III) concentrations were estimated by the difference of both Cr(VI) and total Cr determinations, as previously reported [12]. All sorption experiments were conducted in triplicate to verify the reproducibility of the results, and mean values were informed. Control experiments indicated that no measurable Cr was adsorbed onto the walls of the centrifuge tubes.

2.5. Effect of biosorbent dosage

The influence of biosorbent dosage on the equilibrium adsorption of chromate ions was examined by exposing masses of MFCs ranging from 0.1 to 1 g to 10 mL of a 10 mg/L $\text{K}_2 \text{Cr}_2 \text{O}_7$ solution, shaking at 100 rpm and a constant temperature of 25 °C, until equilibrium was attained. The supernatants' total Cr, Cr(VI), and Cr(III) concentrations were measured as previously described. The experiments were conducted in triplicate to assess reproducibility.

2.6. Influence of pH on Cr(VI) biosorption

Biosorption experiments were conducted using chromium solutions at varying pH levels to identify the pH that resulted in the highest contaminant removal and to assess the impact of this parameter on the biosorbent material. The procedure involved using the 0.08 g/mL biosorbent-solution ratio. The MFCs dosage was then placed in plastic flasks, adding 10 mL of $\text{K}_2 \text{Cr}_2 \text{O}_7$ solution at a 10 mg/L concentration. The pH of each solution was adjusted using 0.1 M HCl or NaOH to achieve values between 2 and 8. The flasks underwent shaking in a thermo-bath with reciprocal motion at a speed of 100 rpm and a temperature of 25 °C until adsorption equilibrium was achieved. Upon completion of the contact period, the solution underwent filtration, and total Cr and Cr(V) concentrations in the supernatant were analyzed as mentioned above.

2.7. Biosorption Isotherms

To determine the influence of concentration on the adsorption process as well as on the equilibrium parameters of the process, batch contact biosorption experiments were carried out between the MFCs and potassium dichromate solutions in a concentration range between 10 to 400 mg/L at different temperatures (25 °C, 35 °C and 45 °C) using the optimum biosorbent dosage and the optimum pH resulting from previous biosorption tests. As previously established, the supernatants were analyzed to determine the concentration of Cr (VI), total chromium, and Cr (III). The tests were also performed in triplicate.

III. RESULTS AND DISCUSSION

3.1. Scanning electron microscopy (SEM)

Figure 1 shows SEM micrographs of cellulose microfibrils (CFMs) obtained from corrugated cardboard waste. In Figure 1a, a complex network of derived cellulose microfibrils can be observed. The fibers are thick and present intertwined structures, indicating that there is not yet a complete separation of individual fibers. The 50 µm scale suggests that these fibers are considerably smaller than those at higher magnification. This micrograph evidences the initial state of the fibers after mechanical and chemical treatment for their production. The presence of grouped fibers could be due to lignin or hemicellulose residues or insufficient pretreatment since these compounds play an important role in plant cell walls' structural organization and properties. Lignin and hemicellulose are essential for the embedding matrix surrounding cellulose microfibrils, influencing their aggregation and structural integrity [17]. Micrographs are relevant to understanding how pretreatment affects fiber dispersion and morphology. It can be established that extraction methods could be optimized to achieve a more homogeneous separation.

On the other hand, Figure 1b, also observed at a magnification of 500x, shows a structure similar to that described above (Figure 1a) but with clearer evidence of fiber fragmentation. The fibers appear more defined and clean, although groupings and certain surface irregularities are still observed. The 50 µm scale maintains the focus on the macrostructure. However, progress in pretreatment is observed in Figure 1a. This fact could indicate a greater degree of defibrillation or purification of the fibers. Surface irregularities could be key sites for applications requiring chemical functionalization or adsorption, such as composite reinforcement processes.

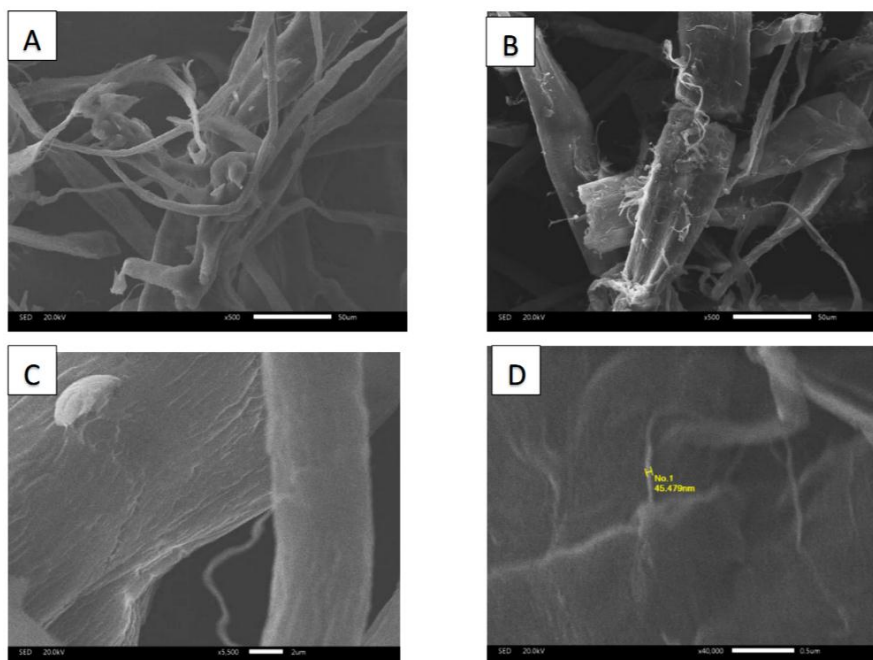


Figure 1: MFCs' SEM micrographs observed at (a) 500x, (b) 500x, (c) 5500x, and (d) 40000x.

Regarding Figure 1c, which was observed at a magnification of 5500x, much finer details of the microfibrils can be seen. The 2 µm scale allows the texture of the fibers to be observed, with folds and a more defined surface. A finer fibrillar structure and some surface defects are noted that could be related to the extraction process; for example, the alkalization process was found to be more effective in removing unwanted substances compared to bleaching, resulting in a more refined fibril structure [18,19]. This magnification reveals how individual fibers show nanometric details in their structure. Imperfections could be indicators of the

mechanical or chemical stress applied during extraction. At this point, the fibers seem ready for deeper analysis, such as crystallinity studies or surface functionalization for specific applications. When the MFCs are observed at a higher magnification (40000x), outstanding details of a cellulose microfibril are observed (Figure 1d). The measurement indicates a thickness of approximately 45.5 nm, confirming the nanometric scale and the presence of some fibers in the biosorbent. The scale of (0.5 μm) clearly reflects the individual separation of the fibrils. A detailed analysis is essential for evaluating the fiber properties at the nanometric level, including their morphology, uniformity, and size. The dimensions obtained indicate that these fibrils could be helpful for advanced applications such as nanocomposites, filtration membranes, or biomedical devices. Direct size measurement supports the characterization and could be correlated with properties such as mechanical strength or surface area.

Figure 2 shows micrographs of the MFCs after the Cr(V) biosorption process. In Figure 2a, the micrograph shows a cellulose microfibrils network with relatively clean and smooth surfaces, although with some roughness and folds. A cross-linked arrangement of the fibers is observed, which indicates a highly porous structure ideal for adsorption processes. Surface roughness can be key for the adsorption of heavy metals, such as chromium, by providing active interaction sites. The porous and cross-linked structure improves the available surface area, facilitating the contact of contaminants with the fiber surface. Figure 2b shows an elemental mapping of the same area of the microfibrils using energy dispersive spectroscopy (EDS). The green color indicates the general distribution of elements detected in the sample. Although the specific elements are not clearly detailed in this micrograph, the presence of carbon, oxygen, nitrogen, sodium, potassium, and chromium can be seen. The MFCs show a predominant composition of carbon, which is the most abundant element in this sample, followed by oxygen and nitrogen, these three elements being part of the original composition of the corrugated cardboard microfibrils. In addition, it reflects a homogeneous surface without significant accumulations of contaminants or other materials. This mapping highlights the ability of the fibers to maintain a uniform distribution of the adsorbed elements after biosorption. Likewise, the homogeneity suggests that the fibers have adequate functionalization or chemical properties that favor balanced adsorption throughout the surface.

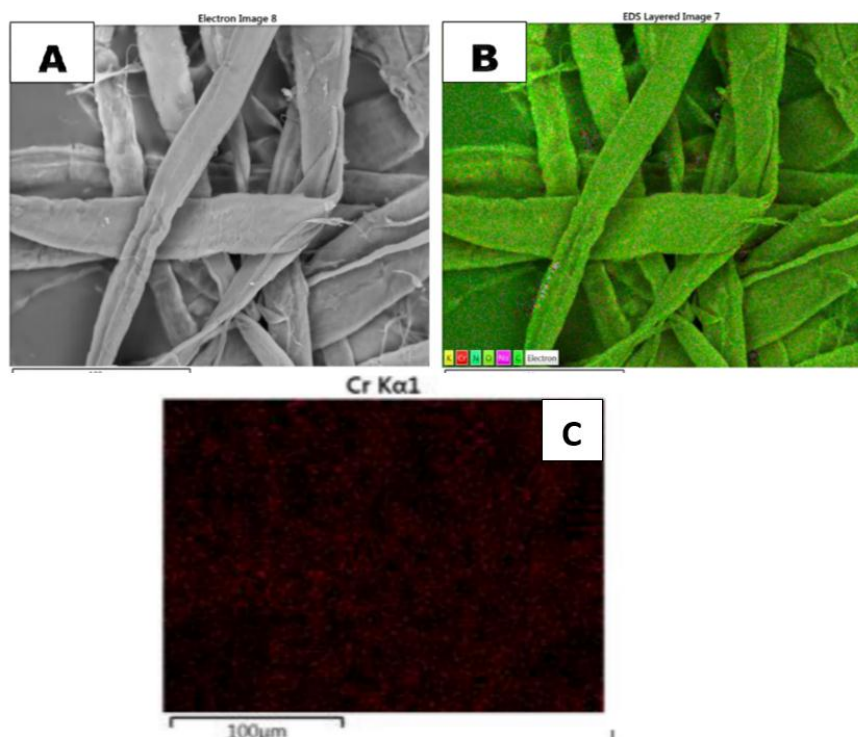


Figure 2: MFCs' SEM micrographs (a) microfibrils observed in the biosorbent structure, (b) elemental mapping of the MFCs, (c) chromium content in MFCs after biosorption.

On the other hand, Figure 2 corresponds to the elemental mapping of chromium in the fibers after the biosorption process. The distribution of chromium (indicated by the red dots) is dispersed along the entire surface of the microfibrils. No massive accumulations are observed at specific points, suggesting uniform adsorption. The 100 μm scale covers a wide area, showing that the biosorption process occurred at a macroscopic level. This mapping confirms that cellulose microfibrils are capable of efficiently adsorbing

chromium. The uniform distribution indicates that the material has a high affinity towards chromium, probably due to functional groups on the surface (such as hydroxyls or carboxyls) that interact with chromium ions. This result is significant in water treatment applications, as it suggests that the adsorbent can capture chromium without becoming quickly saturated at specific points. Finally, it can be established that the porous structure in Figure 2a and the homogeneous distribution of chromium in Figure 2c make these fibers an effective biosorbent for heavy metals, particularly Cr(VI), which forms oxyanions in aqueous solutions. This research has direct practical applications, as these fibers can be used in water treatment systems to remove chromium from industrial effluents, particularly in chrome plating or leather tanning processes.

3.2. Fourier-Transform Infrared analyses (FTIR)

Figure 3 shows the FTIR analyses of the MFC samples before (red line) and after Cr(VI) biosorption (black line). Before biosorption (MFCs), a broad and strong band around $3300\text{--}3400\text{ cm}^{-1}$ is observed, attributed to stretching vibrations of the hydroxyl groups (-OH); this reflects the presence of hydrogen bonds characteristic of cellulose fibers. The presence of a small peak in the region of 2900 cm^{-1} is related to the C-H stretching of the bonds in the methyl and methylene groups (-CH₂ and -CH₃). After biosorption (MFCs-Cr), the intensity of the band corresponding to the -OH group decreases markedly, indicating that the hydroxyl groups participated in the interaction with chromium ions, probably by forming coordination bonds or through proton substitution. These groups provide active sites for the binding of chromium ions, facilitating their removal from solutions [20,21]. Furthermore, the decrease in the C-H intensity indicates that the methyl and methylene groups were able to experience some degree of interaction with the chromium ions, although to a lesser extent than the -OH.

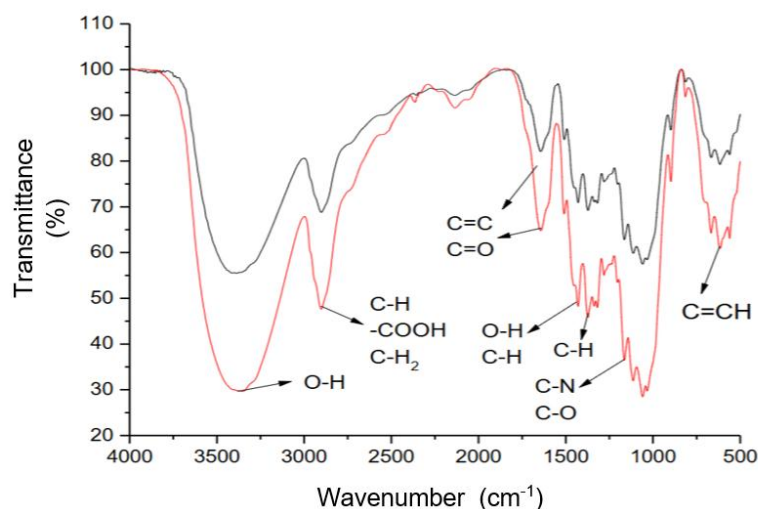


Figure 3: FTIR spectra of MFC (red line) and MFCs after chromium biosorption (black line).

Furthermore, a peak at $1730\text{--}1740\text{ cm}^{-1}$ in MFCs indicates the presence of carbonyl (C=O) stretching vibrations of carboxyl groups (-COOH) or esters. This functional group is important for metal adsorption due to its electron-donating ability. A band around 1600 cm^{-1} is also attributed to C=C bonds of aromatic rings or vibrations associated with conjugated groups. After biosorption, the C=O peak in Cr-MFCs slightly shifts to a lower wavelength (ca. 1710 cm^{-1}), suggesting complex formation between carbonyl groups and chromium. Likewise, the change in the intensity of the peaks at 1600 cm^{-1} confirms interactions with the C=C, indicating that chromium could have formed coordination bonds with these groups, as well as physisorption mechanisms [22].

In the spectrum of MFCs, multiple bands are observed in this region, associated with C-H bond deformation vibrations at $1400\text{--}1450\text{ cm}^{-1}$, C-O stretching vibrations at $1100\text{--}1200\text{ cm}^{-1}$, characteristic of the glycosidic units of cellulose, and also the presence of C-N bonds around 1300 cm^{-1} , if residual nitrogen impurities are present. On the other hand, in the MFCs-Cr spectrogram, the intensity of the peaks at $1300\text{--}1400\text{ cm}^{-1}$ increases, suggesting the interaction of chromium with C-H or C-N bonds, probably forming coordination bonds. The peaks in the $1100\text{--}1200\text{ cm}^{-1}$ (C-O) region also decrease in intensity, indicating that these functional groups participated in the biosorption.

The region below 1000 cm^{-1} is dominated by peaks associated with out-of-plane deformation vibrations of C=CH and C-O bonds of cellulose. After biosorption, an increase in the intensity of the peaks at $600\text{--}800\text{ cm}^{-1}$ is observed, which can be attributed to the interactions of chromium with C=CH bonds and deformations of aromatic rings, suggesting an adsorption process in these regions.

In general, the predominant interactions of chromium with the functional groups of MFCs can be established with the key functional groups in biosorption, such as hydroxyls (-OH), carboxyls (-COOH), carbonyls (C=O) and C-O bonds of cellulose. These groups acted as active sites for the binding of chromium ions. In addition, the shift of the FTIR bands after biosorption confirms that the interaction is chemical, probably through the formation of coordination bonds. The suggested mechanism of chromium biosorption, based solely on FTIR results, suggests that it occurs primarily via chemisorption, where chromium ions form covalently coordinated bonds with the functional groups of cellulose. The decrease in the intensity of the -OH and C=O peaks suggests that these functional sites are primarily responsible for the process. These results confirm the potential of cellulose microfibers as effective biosorbents for chromium. Furthermore, additional functionalization of the material could further optimize its adsorption capacity.

3.3. Zeta potential

The zeta potential (ξ) versus pH plot of the MFCs is shown in Figure 4, combined with the point of zero charge analysis ($\text{pH}_{\text{PZC}} \sim 7.8$). This plot provides crucial information about their performance as biosorbents for hexavalent chromium removal in aqueous solutions. For example, in the acidic region ($\text{pH} < \text{pH}_{\text{PZC}}$), the surface of the MFCs is positively charged due to the protonation of functional groups such as hydroxyl groups (-OH): protonated at low pH; carboxyl groups (-COOH) are not dissociated, contributing to the overall positive charge. This positive state favors the electrostatic attraction of the predominant Cr(VI) anions, such as $\text{Cr}_2\text{O}_7^{2-}$ and CrO_4^{2-} , present in acidic solutions. At pH close to 4-5, the zeta potential is higher (+50 mV), suggesting a higher affinity of the MFCs towards anionic species, maximizing the removal efficiency. Also, at pH_{PZC} (~7.8), the surface of the MFCs has no net charge, which implies a significant reduction in the electrostatic interactions between the microfibers and the Cr(VI) anions. At this point, removing Cr(VI) is probably based on additional mechanisms, such as specific chemical interactions (formation of bonds with functional groups).

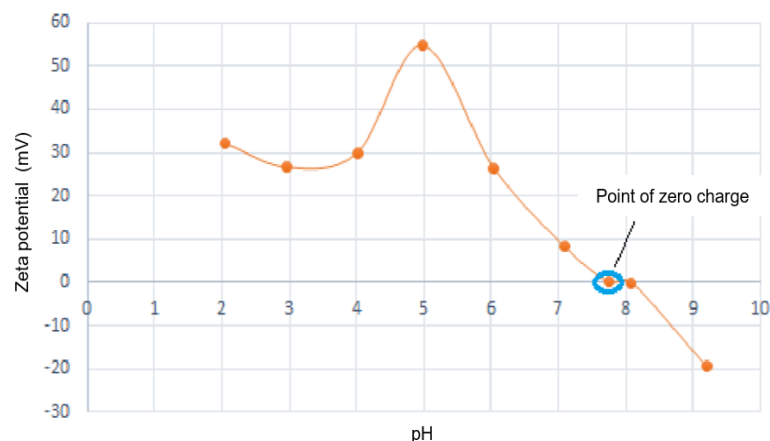


Figure 4: FTIR spectra of MFC (red line) and MFCs after chromium biosorption (black line).

On the other hand, analyzing the basic (alkaline) region ($\text{pH} > \text{pH}_{\text{PZC}}$), at pH higher than 7.8, the surface of the MFCs acquires a negative charge due to the dissociation of functional groups such as carboxyls (-COOH \rightarrow $-\text{COO}^-$) and phenols (-OH \rightarrow $-\text{O}^-$). In this range, electrostatic interactions with Cr(VI) anions become unfavorable. However, chromium can be present as Cr^{3+} in basic environments, allowing some adsorption through electrostatic attraction and bond formation with the functional groups of MFCs. These results suggest mechanisms for Cr(VI) removal by MFCs, which depend on both electrostatic interactions and chemical mechanisms depending on pH.

Furthermore, it could be predicted that the acidic pH range, especially between 4–6, is the most effective for Cr(VI) biosorption since the dominant Cr(VI) species in acidic solutions ($\text{Cr}_2\text{O}_7^{2-}$ and HCrO_4^-) are highly reactive with positively charged surfaces. Likewise, at acidic pH, the reduction of Cr(VI) to Cr(III) can occur through redox processes facilitated by the electrons available in MFCs or reactive species in solution. This phenomenon is crucial to immobilize Cr in less toxic and more stable forms. MFCs, having a well-defined pH_{PZC} , are suitable for designing Cr(VI) removal systems with pH adjustments that optimize the anionic interaction. Furthermore, pH control can ensure high adsorption efficiency, particularly in the acidic range. Zeta potential evaluation suggests that MFCs not only act as biosorbents but also offer the possibility of modifying their surface to improve their adsorption capacity, expanding their applicability in wastewater treatment.

3.4. Kinetic experiments

Figure 5 shows the kinetics of chromium biosorption by MFCs. The removal of total chromium, Cr(VI), and Cr(III) were plotted. It can be observed that both the removal of Cr(VI) and total chromium are quite similar. For example, the removal of total chromium starts around 45% and shows an initial increase until approximately 60 minutes, reaching a peak close to 60% removal; after this peak, the removal of total chromium stabilizes around 50-55% until 120 minutes. While the removal of Cr(VI) (blue line) starts at around 40% and shows a relatively stable behavior with slight fluctuations over time, the removal of Cr(VI) remains in a range of 40-45%. Although there are differences in removal percentages between total chromium and Cr(VI), it can be concluded that they refer to the same type of chemical species that MFCs target for removal. These differences can be attributed to the analytical method of determining total Cr and Cr(VI).

On the other hand, the removal of Cr(III) is observed to be practically zero during the entire period evaluated. This fact indicates that there is no significant reduction of Cr(VI) to Cr(III) since the yellow line (Cr(III)) remains at 0% during the entire time. Therefore, it is concluded that cellulose microfibrils do not promote the reduction of Cr(VI) to Cr(III) under the conditions evaluated. Likewise, it can be established that the MFCs obtained from corrugated cardboard waste show a significant capacity to adsorb total chromium, reaching up to 60% removal. However, the lack of reduction of Cr(VI) to Cr(III) could limit its application in processes where Cr(VI) reduction is crucial due to the toxicity of Cr(VI) compared to Cr(III). Finally, chromium removal using cellulose microfibrils (CFMs) can be considered relatively fast compared to other biosorbents (Tejada Tovar). However, the removal rate may vary depending on factors such as pH, initial chromium concentration, amount of CFMs used, and solution conditions.

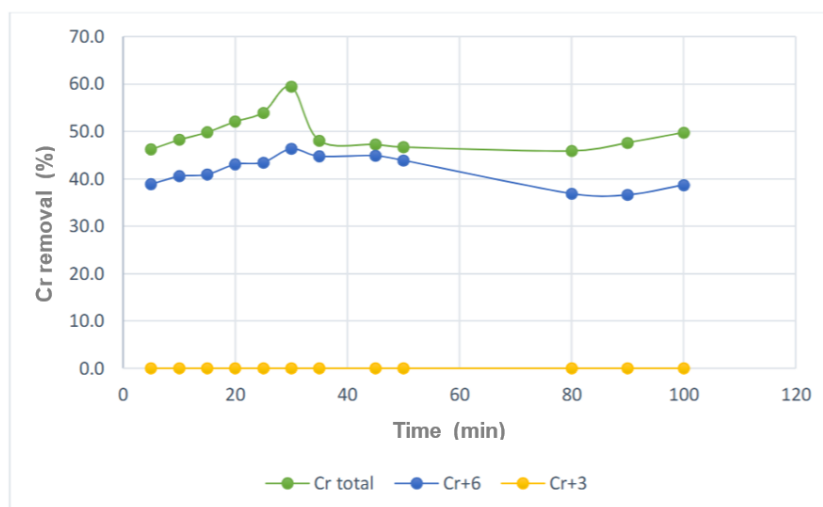


Figure5: Chromium removal as a function of time using MFCs as biosorbent.

3.5. Effect of biosorbent dosage

Figure 6 shows the chromium biosorption by MFCs at different biosorbent doses. Similarly, the reduction of Cr(VI) to Cr(III) was evaluated, and the total chromium removal was plotted. Total Cr removal starts at around 45% at low MFC concentrations (0.01 g/mL). As the dose increases, total Cr removal gradually increases, reaching approximately 60% at a 0.1 g/mL concentration. This indicates that a higher amount of biosorbent improves the total chromium removal capacity in the solution. Cr(VI) removal starts at around 40% at low MFC concentrations; it remains relatively constant up to a concentration of approximately 0.06 g/mL, where it starts to increase, reaching about 50% at 0.1 g/mL. This suggests that MFCs effectively remove Cr(VI), especially at higher doses.

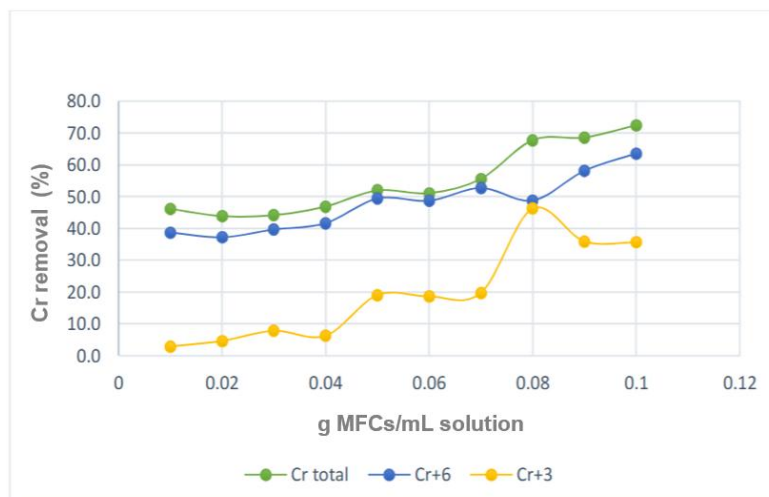


Figure 6: Effect of dosage on chromium removal using MFCs as biosorbent.

On the other hand, in this case, a reduction of Cr(VI) is observed since the removal of Cr(III) starts very low, around 10%, at low doses of MFCs. As the dose of MFCs increases, the removal of Cr(III) also increases, reaching a peak close to 30% at a concentration of 0.06 g/mL. However, after this point, the removal of Cr(III) decreases slightly, stabilizing around 20% at higher concentrations of MFCs. This behavior may indicate an initial reduction of Cr(VI) to Cr(III), followed by a lower efficiency in the removal of Cr(III) at higher doses. The graph suggests a reduction of Cr(VI) to Cr(III) at higher doses of MFCs. This can be inferred from the increase in Cr(III) removal up to a concentration of 0.06 g/mL, followed by a stabilization or slight decrease. Cr(VI) removal increases with the MFCs dose, indicating that MFCs not only adsorb Cr(VI) but may also be facilitating its reduction to Cr(III). The difference in the Cr(VI) and Cr(III) removal curves at different MFC doses supports the hypothesis that MFCs promote the reduction of Cr(VI) to Cr(III), especially at higher doses. Cellulose microfibrils (MFCs) have a good adsorption capacity for hexavalent chromium, with maximum Cr(VI) removal reaching about 50% at a 0.06 g/mL dose. The reduction of Cr(VI) to Cr(III) showed a peak at this dose, suggesting the most effective reduction of Cr(VI) to Cr(III) in this range. This dose is considered a balance point, allowing for high efficiency in total chromium removal and effectively reducing Cr(VI) to Cr(III) without saturating quickly. Based on the above, cellulose microfibrils obtained from corrugated cardboard waste effectively remove chromium from aqueous solutions with higher efficiency at higher biosorbent doses. In addition, there are indications that MFCs facilitate the reduction of Cr(VI) to Cr(III), which is beneficial for detoxifying chromium-contaminated waters.

3.6. Influence of pH on Cr(VI) biosorption

Figure 7 shows a graph of chromium removal as a function of pH using MFCs. The graph presents three curves representing the removal of total chromium (total Cr), hexavalent chromium (Cr(VI)), and trivalent chromium (Cr(III)) at different pH values. It can be observed that total chromium removal is high (around 90-100%) at low pH values (pH 2). As the pH increases, total chromium removal decreases dramatically and stabilizes around 50% for pH between 4 and 9. Regarding Cr(VI) removal, it is lower than total and Cr(III) removal. At low pH (pH 2), removal is approximately 60-70%. From pH 3 onwards, removal decreases and stabilizes around 40% for pH between 4 and 9. While, for Cr(III), biosorption follows a similar trend as for total chromium: At low pH (pH 2), removal is high (around 90-100%), and as pH increases, removal decreases and stabilizes around 30-40% for pH between 4 and 9. The graph suggests that there is a reduction of Cr(VI) to Cr(III) at low pH values (0-2) since Cr(III) removal is significantly high at these pH values. The reduction of Cr(VI) at low pH values in biosorbents is primarily driven by the enhanced availability of protons [23], which facilitate the reduction process, and the increased activity of functional groups on biosorbents that interact with Cr(VI). At low pH, the acidic environment provides a conducive setting for reducing Cr(VI) to Cr(III), a less toxic form. As pH increases, Cr(VI) and Cr(III) removal stabilize at lower values, indicating that Cr(VI) reduction to Cr(III) is less efficient at higher pHs. This graph is relevant because it shows how pH affects the efficiency of chromium biosorption using MFCs, which is crucial to optimize treatment processes for chromium-contaminated waters.

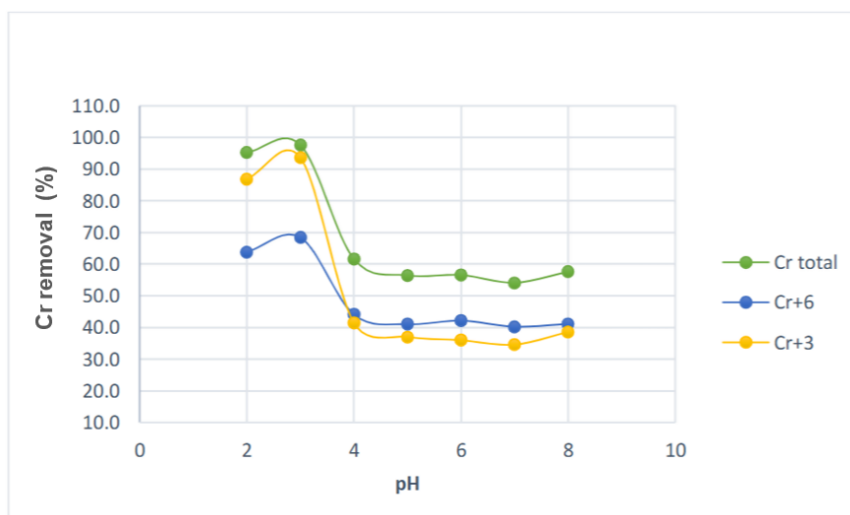


Figure7: Influence of pH on chromium removal using MFCs as biosorbent.

3.7. Influence of pH on Cr(VI) biosorption

The biosorption isotherms of Cr(VI) by cellulose microfibrils (CFMs) obtained from corrugated cardboard waste at different temperatures (25°C, 35°C and 45°C) are shown in Figure 8, where the equilibrium concentration of Cr(VI) (C_e) in mg Cr⁶⁺ /L is plotted versus the concentration of Cr(VI) on the adsorbent at equilibrium (q_e) in mg Cr⁶⁺ /g CFM. The isotherm at 25°C shows an initial increase in biosorption capacity (q_e) as the equilibrium concentration (C_e) increases, reaching a peak around 50 mg Cr⁶⁺ /L with a biosorption capacity of approximately 400 mg Cr⁶⁺ /g MFC. After this peak, the biosorption capacity decreases slightly and increases again more sharply at higher equilibrium concentrations, reaching a maximum value of approximately 800 mg Cr⁶⁺ /g MFC. The isotherm at 35°C follows a similar trend as at 25°C but with a slightly higher biosorption capacity overall. The initial peak is observed around 50 mg Cr⁶⁺ /L with a biosorption capacity of approximately 450 mg Cr⁶⁺ /g MFC. The biosorption capacity decreases slightly after the initial peak and then increases more sharply, reaching a maximum value of approximately 900 mg Cr⁶⁺ /g MFC. The isotherm at 45°C shows a significantly lower biosorption capacity than the other two temperatures. The biosorption capacity increases gradually and does not exhibit a pronounced peak like at other temperatures. The maximum biosorption capacity at 45°C is approximately 300 mg Cr⁶⁺ /g MFC. This behavior may be due to damage to the structure of MFCs due to high temperatures. It is also concluded that as the temperature increases from 25°C to 35°C, the Cr(VI) biosorption capacity also increases, suggesting that biosorption is more efficient at higher temperatures within this range. However, at 45°C, the biosorption capacity decreases significantly, indicating that high temperatures may not favor Cr(VI) biosorption by MFCs. This information is relevant for optimizing Cr(VI) biosorption conditions using MFCs, as it identifies the optimal temperature to maximize adsorption capacity.

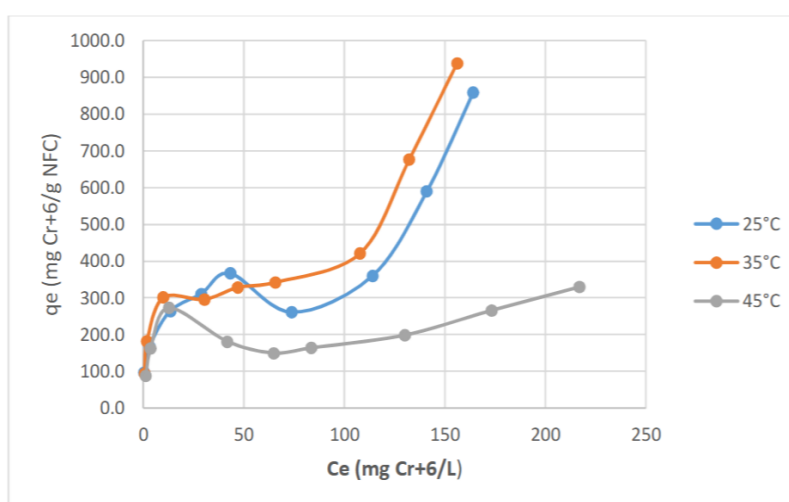


Figure8: Cr(VI) biosorption isotherms using MFCs as biosorbents at different temperatures.

IV. CONCLUSIONS

The study aimed to explore the potential of cellulose microfibers (MFCs) derived from corrugated cardboard waste as a sustainable biosorbent for removing hexavalent chromium (Cr(VI)) from aqueous solutions. The results confirmed the hypothesis, revealing MFCs to have favorable physicochemical properties for Cr(VI) biosorption and reduction. The study found that MFCs had a high surface-to-volume ratio, abundant functional groups, and a porous structure, contributing to their adsorption capacity. FTIR analysis revealed that these groups were crucial in binding Cr(VI) ions and reducing them to less toxic Cr(III). The experimental findings showed a high adsorption capacity of approximately 900 mg Cr(VI)/g at 35°C and efficient biosorption under acidic conditions. Kinetic studies showed rapid Cr(VI) adsorption within the first hour, and isotherm analysis revealed MFCs as sustainable alternatives to conventional adsorbents. MFCs also demonstrated their dual role as adsorbents and reducing agents, demonstrating their potential for environmental remediation. The study advances waste-derived materials for environmental remediation and aligns with circular economy principles.

ACKNOWLEDGMENTS

The authors acknowledge the financial support provided by Coordinación de la Investigación Científica-UMSNH, Grant CIC-UMSNH-2024, and are grateful to the technical support of Selene A. Valencia-Leal and Dulce M. Bocanegra-Ramírez.

REFERENCES

- [1] Arora V, Bithel N, Singh R. A Study on Heavy Metal Sources and Pollution: Challenge to Biological and Ecosystem. | EBSCOhost 2023;42B:44. <https://doi.org/10.48165/bpas.2023.42B.1.7>.
- [2] Adnan M, Xiao B, Ali MU, Xiao P, Zhao P, Wang H, et al. Heavy metals pollution from smelting activities: A threat to soil and groundwater. *Ecotoxicology and Environmental Safety* 2024;274:116189. <https://doi.org/10.1016/j.ecoenv.2024.116189>.
- [3] Velayatzadeh M. Heavy Metals in Surface Soils and Crops. *Heavy Metals - Recent Advances*, IntechOpen; 2023. <https://doi.org/10.5772/intechopen.108824>.
- [4] Gogoi B, Acharjee SA, Bharali P, Sorhie V, Walling B, Alemtoshi. A critical review on the ecotoxicity of heavy metal on multispecies in global context: A bibliometric analysis. *Environmental Research* 2024;248:118280. <https://doi.org/10.1016/j.envres.2024.118280>.
- [5] Singh V, Singh N, Verma M, Kamal R, Tiwari R, Sanjay Chivate M, et al. Hexavalent-Chromium-Induced Oxidative Stress and the Protective Role of Antioxidants against Cellular Toxicity. *Antioxidants* 2022;11:2375. <https://doi.org/10.3390/antiox11122375>.
- [6] Madumo TM. Industrial Wastewater Treatment Past and Future Perspectives in Technological Advances for Mitigation of Cr(VI) Pollutant. *IntechOpen*; 2024. <https://doi.org/10.5772/intechopen.1004933>.
- [7] Vyas RN, Brankle D, Howell J. Determination of Cr(VI) in Natural and Waste Waters Using Differential Pulse Polarography According to U.S. Epa (SW-846 Method 7198). *Meet Abstr* 2022;MA2022-01:2443. <https://doi.org/10.1149/MA2022-01512443mtgabs>.
- [8] Das BK, Das PK. Green technology to limit the effects of hexavalent chromium contaminated water bodies on public health and vegetation at industrial sites n.d.
- [9] Rama Devi D, Srinivasan G, Kothandaraman S, Ashok Kumar S. State-of-the-Art Review—Methods of Chromium Removal from Water and Wastewater. In: Ramanagopal S, Gali ML, Venkataraman K, editors. *Sustainable Practices and Innovations in Civil Engineering*. Singapore: Springer; 2021, p. 37–51. https://doi.org/10.1007/978-981-15-5101-7_4.
- [10] Peng H, Guo J. Removal of chromium from wastewater by membrane filtration, chemical precipitation, ion exchange, adsorption electrocoagulation, electrochemical reduction, electro dialysis, electrodeionization, photocatalysis and nanotechnology: a review. *Environ Chem Lett* 2020;18:2055–68. <https://doi.org/10.1007/s10311-020-01058-x>.
- [11] Liu B, Xin Y-N, Zou J, Khoso FM, Liu Y-P, Jiang X-Y, et al. Removal of Chromium Species by Adsorption: Fundamental Principles, Newly Developed Adsorbents and Future Perspectives. *Molecules* 2023;28:639. <https://doi.org/10.3390/molecules28020639>.
- [12] Ortíz-Gutiérrez M, Alfaro-Cuevas-Villanueva R, Martínez-Miranda V, Hernández-Cristóbal O, Cortés-Martínez R. Reduction and Biosorption of Cr(VI) from Aqueous Solutions by Acid-Modified Guava Seeds: Kinetic and Equilibrium Studies. *Polish Journal of Chemical Technology* 2020;22:36–47. <https://doi.org/10.2478/pjct-2020-0037>.
- [13] Ramos-Vargas S, Huirache-Acuña R, Guadalupe Rutiaga-Quiñones J, Cortés-Martínez R. Effective lead removal from aqueous solutions using cellulose nanofibers obtained from water hyacinth. *Water Supply* 2020;20:2715–36. <https://doi.org/10.2166/ws.2020.173>.
- [14] Kumar V, Pathak P, Bhardwaj NK. Waste paper: An underutilized but promising source for nanocellulose mining. *Waste Management* 2020;102:281–303. <https://doi.org/10.1016/j.wasman.2019.10.041>.
- [15] Vázquez-Guerrero A, Cortés-Martínez R, Alfaro-Cuevas-Villanueva R, Rivera-Muñoz EM, Huirache-Acuña R. Cd(II) and Pb(II) Adsorption Using a Composite Obtained from Moringa oleifera Lam. Cellulose Nanofibrils Impregnated with Iron Nanoparticles. *Water* 2021;13:89. <https://doi.org/10.3390/w13010089>.
- [16] Wang H, Li D, Zhang R. Preparation of Ultralong Cellulose Nanofibers and Optically Transparent Nanopapers Derived from Waste Corrugated Paper Pulp. | EBSCOhost 2013;8:1374. <https://doi.org/10.15376/biores.8.1.1374-1384>.
- [17] Li H, Chen B, Kulachenko A, Jurkane V, Mathew AP, Sevastyanova O. A comparative study of lignin-containing microfibrillated cellulose fibers produced from softwood and hardwood pulps. *Cellulose* 2024;31:907–26. <https://doi.org/10.1007/s10570-023-05674-y>.
- [18] Chalid N Hari Eko Irianto, Rini Riastuti, Azizah Intan Pangesty, Adam F Nugraha, Mitsugu Todo, Aidah Jumahat, Mochamad. Extraction and Characterization of Micro-fibrillated Cellulose from Rice Husk Waste for Biomedical Purposes. *IJTech - International Journal of Technology* n.d. <https://ijtech.eng.ui.ac.id/article/view/6698> (accessed December 7, 2024).
- [19] Hanafiah SF, Danial WH, Samah MAA, Samad WZ, Susanti D, Salim RM, et al. EXTRACTION AND CHARACTERIZATION OF MICROFIBRILLATED AND NANOFIBRILLATED CELLULOSE FROM OFFICE PAPER WASTE 2019;23.

- [20] Khatri GG, Baskota M, Chand A, Bharati S, Paudel DR. Biosorption study of Cr (VI) from the aqueous solution using chemically modified biomass of a newly isolated edible mushroom waste. *BIBECHANA* 2024;21:221–32. <https://doi.org/10.3126/bibechana.v21i3.62097>.
- [21] Gunatilake S. Removal of Cr (III) Ions from Wastewater using Sawdust and Rice Husk Biochar Pyrolyzed at Low Temperature. *International Journal of Innovation Education and Research* 2016;4:44–54. <https://doi.org/10.31686/ijer.vol4.iss4.531>.
- [22] Fernández-Pezua M, Lavado-Meza C, De la Cruz-Cerrón L, Gamarra-Gómez F, Sacari-Sacari E, Lavado-Puente C, et al. Biosorption of Cr(VI) by *Theobroma cacao* pericarp. *Environ Sci Pollut Res* 2024;31:59700–11. <https://doi.org/10.1007/s11356-024-34971-7>.
- [23] Tan A, Wang H, Zhang H, Zhang L, Yao H, Chen Z. Reduction of Cr(VI) by *Bacillus toyonensis* LBA36 and its effect on radish seedlings under Cr(VI) stress. *PeerJ* 2024;12:e18001. <https://doi.org/10.7717/peerj.18001>.